

Heterogeneous Distributed Lag Models to Estimate Personalized Effects of Maternal Exposures to Air Pollution

Daniel Mork*

Department of Statistics, Colorado State University

Marianthi-Anna Kioumourtzoglou

Department of Environmental Health Sciences

Columbia University Mailman School of Public Health

Marc Weisskopf

Department of Environmental Health

Harvard T.H. Chan School of Public Health

Brent A Coull

Department of Biostatistics

Harvard T.H. Chan School of Public Health

Ander Wilson

Department of Statistics, Colorado State University

September 29, 2021

*This work was supported by National Institutes of Health grants ES029943, ES028811, and P30-ES000002. This research was also supported by USEPA grants RD-839278 and RD-83587201. Its contents are solely the responsibility of the grantee and do not necessarily represent the official views of the USEPA. Further, USEPA does not endorse the purchase of any commercial products or services mentioned in the publication. This work utilized the RMACC Summit supercomputer, which is supported by the National Science Foundation (awards ACI-1532235 and ACI-1532236), the University of Colorado Boulder and Colorado State University. The RMACC Summit supercomputer is a joint effort of the University of Colorado Boulder and Colorado State University. These data were supplied by the Center for Health and Environmental Data Vital Statistics Program of the Colorado Department of Public Health and Environment, which specifically disclaims responsibility for any analyses, interpretations, or conclusions it has not provided.

Abstract

Children’s health studies support an association between maternal environmental exposures and children’s birth and health outcomes. A common goal in such studies is to identify critical windows of susceptibility — periods during gestation with increased association between maternal exposures and a future outcome. The associations and timings of critical windows are likely heterogeneous across different levels of individual, family, and neighborhood characteristics. However, the few studies that have considered effect modification were limited to a few pre-specified subgroups. We propose a statistical learning method to estimate critical windows at the individual level and identify important characteristics that induce heterogeneity. The proposed approach uses distributed lag models (DLMs) modified by Bayesian additive regression trees to account for effect heterogeneity based on a potentially high-dimensional set of modifying factors. We show in a simulation study that our model can identify both critical windows and modifiers responsible for DLM heterogeneity. We estimate the relationship between weekly exposures to fine particulate matter during gestation and birth weight in an administrative Colorado birth cohort. We identify maternal body mass index (BMI), age, Hispanic designation, and education as modifiers of the distributed lag effects and find non-Hispanics with increased BMI to be a susceptible population.

Keywords: environmental exposures, critical windows of susceptibility, distributed lag models, effect heterogeneity, Bayesian additive regression trees

1 Introduction

A growing body of research has found maternal exposure to environmental chemicals during pregnancy to be associated with changes in children’s birth and health outcomes. Detrimental outcomes linked to increased exposure include decreased birth weight (Bell et al., 2007), increased risk of preterm birth (Stieb et al., 2012), increased risk of asthma (Lee et al., 2017; Bose et al., 2017), and altered neurological outcomes (Chiu et al., 2016), among others (Šrám et al., 2005). Recently, research has focused on determining the time periods during fetal development, or critical windows of susceptibility, when increased exposure can alter future health outcomes. Identification of critical windows gives insight into how biological processes involved in development may be impacted by exposure to environmental chemicals (Wright, 2017). However, exposure effects, including critical window timing and effect magnitude, are likely to vary across a population. Effect heterogeneity may be governed by biological (e.g., sex of child), socioeconomic (e.g., maternal income), or other non-chemical environmental factors (e.g., neighborhood characteristics). Estimating individualized exposure effects will better inform precision environmental health interventions. Furthermore, this brings attention to vulnerable populations, which the Environmental Protection Agency (EPA) is required to protect through the 2016 update to the Toxic Substances Control Act (Krimsky, 2017).

A commonly applied method to identify perinatal critical windows and estimate the exposure-response relation between maternal exposures and an outcome is the distributed lag model (DLM). In a DLM, an outcome is regressed on repeated measures of an exposure assessed over a time period prior to the outcome. DLMs are typically constrained so the exposure-response function varies smoothly over the time period of exposure. These constraints yield effect estimates that are more biologically plausible as well as add stability to the estimator in the presence of high autocorrelation in the exposure data, which is typical with repeated measures of environmental exposures, such as the air pollution exposure considered in this paper. Methods for constraining DLMs include splines (Zanobetti et al., 2000; Gasparrini et al., 2010), Gaussian processes (Warren et al., 2012), principal components (Wilson et al., 2017), and regression trees (Mork and Wilson, 2021a). The majority of studies that apply these methods assume a homogeneous exposure-response relationship across the population.

Several methods have sought to estimate DLMs that vary across a population. Wilson et al. (2017) proposed a Bayesian distributed lag interaction model (BDLIM) to estimate differences in the exposure-response function for a parsimonious set of predetermined subgroups. Warren et al. (2012) and Warren et al. (2020) developed spatially-varying DLMs to account for changes in pollution composition or demographics over a study region. These papers highlight the bias incurred by a homogeneous effects assumption when effects are

truly heterogeneous. BDLIM has been applied in several epidemiological analyses, including two that found an increased risk of asthma due to prenatal exposures to fine particulate matter and nitrate for a subgroup of boys concurrently exposed to high prenatal stress (Lee et al., 2017; Bose et al., 2017). Despite these advances in estimating DLM heterogeneity, the methods of Wilson et al. (2017), Warren et al. (2012), and Warren et al. (2020) remain limited in their scope and interpretability. A spatially-varying DLM is unable to identify the subject characteristics associated with changes in the underlying distributed lag function. BDLIM is limited to predefined categorical subgroups and is most reasonably applied to data having only a small number of subgroups. In the age of big data, we have access to a potentially high dimensional set of categorical and continuous modifiers, and the true modifiers responsible for differences in distributed lag effects are unknown. Harnessing this information can lead to personalized environmental health decision making.

We propose a Bayesian additive regression tree (BART) method for estimating distributed lag effect heterogeneity due to a set of modifying covariates. The BART framework of Chipman et al. (2010) is a popular method for estimating non-parametric functions. Extensions of BART allow for estimating distributed lag nonlinear (Mork and Wilson, 2021b) and mixture models (Mork and Wilson, 2021a). The treed DLM approach of Mork and Wilson (2021a) outperforms competing spline and Gaussian process methods when the goal is distributed lag effect estimation and critical window identification. However, both of these approaches assume a common distributed lag effect for all individuals.

Chipman et al. (2002) proposed treed regression models that modify a vector of regression coefficients using a single Bayesian tree. More recently, several approaches have used an ensemble of multiple Bayesian trees to modify a single predictor. For example, Starling et al. (2020) introduced BART with targeted smoothing (tsBART), which allows a smooth risk function of a single univariate predictor to vary across a population. Deshpande et al. (2020) proposed a varying coefficient BART model that uses a separate ensemble of regression trees to modify each regression coefficient in the model. In a non-Bayesian approach to estimating effect heterogeneity, Odden et al. (2020) applied a random forest algorithm to identify heterogeneous exposure associations. However, no method has been proposed to modify a structured vector of regression coefficients, such as a constrained distributed lag function, using an ensemble of trees.

In this paper, we define the heterogeneous DLM (HDLM). HDLM extends the DLM to estimate a personalized distributed lag function that varies across the population according to a possibly high dimensional set of potential modifying factors. Our additive regression tree method introduces individualized functional predictors through a vector of structured regression coefficients on the terminal nodes of a modifier tree. Specifically, an ensemble of regression trees divides the sample based on a set of modifying covariates and estimates a

DLM unique to each subgroup. We introduce three methods for estimating the distributed lag effects on the modifier tree terminal nodes. The first considers a Gaussian process DLM for each subgroup and assumes the same smoothness in the distributed lag effects for all observations. The second method incorporates the treed DLM method of Mork and Wilson (2021a) and defines a nested tree structure where the treed DLM is used to estimate unique critical windows and effect sizes for the subgroup at each terminal node of the modifier tree. This approach relaxes the smoothness assumption imposed by Gaussian processes and improves performance when the magnitude of the effect varies over the population or there are subgroups with no exposure effect. The third method also uses a treed DLM whose structure is shared across all subgroups and allows for variation in only the magnitude of the effect, but not the location of the critical window. This approach shares information on the structure of the DLM across subgroups. We develop a computational framework for our methods that selects modifying covariates responsible for changes in the exposure-response relationship. In addition, our method extends the tree literature by introducing the concept of a nested tree model, where a tree-based functional estimator is given to subgroups defined by a traditional regression tree.

We provide a comprehensive simulation of our method and show it is able to estimate individualized critical windows and effects as well as identify the covariates responsible for modifying the distributed lag function. The simulation also shows that the nested and shared tree HDLMs outperform the Gaussian Process HDLM in terms of HDLM estimation and critical window detection. We apply our method to a Colorado-based administrative birth cohort and explore differences in the relationship between fine particulate matter ($PM_{2.5}$) and birth weight across a range of continuous, categorical, and binary modifiers specific to individuals. We identify age, body mass index (BMI), Hispanic designation, and education as potential modifiers of the distributed lag effects. The analysis indicates that non-Hispanics with increased BMI are more susceptible to $PM_{2.5}$ exposures and early- and late-gestation are potential critical windows. In addition, we find individual variability within subgroups due to other modifying characteristics. Software to replicate our simulation and use our method in other applications is available in the R package `dlmtree`.

2 Colorado Birth Cohort Data

We analyze birth weight for gestational age z -score (BWGAZ) using birth vital statistics records from Colorado, USA. BWGAZ is the birth weight adjusted for gestational age and fetal sex using a standard reference table (Fenton and Kim, 2013). Besides birth outcomes, the data include individual covariate information including mother’s age, weight, height, income, education, marital status, prenatal care habits, smoking before and during

pregnancy, as well as race and Hispanic designations. The data include all births from Colorado with estimated conception dates between 2007 and 2015, inclusive. We limit the data to the northern front range counties (those immediately east of the Rocky Mountains roughly extending from Colorado Springs to the Wyoming border). This area contains the majority of the Colorado population. We further restrict our analysis to census tracts with elevation lower than 6000 feet above sea level. This restriction both reduces the potential confounding by altitude and the impact of mountainous terrain on exposure data. We analyze singleton, full-term births (≥ 37 weeks) with complete covariate and exposure data, resulting in 310,236 births.

We are interested in the association between a mother’s weekly exposure to particulate matter smaller than or equal to $2.5\mu\text{m}$ in diameter ($\text{PM}_{2.5}$) and resulting birth weight. In addition, we wish to identify vulnerable populations with increased susceptibility to $\text{PM}_{2.5}$ exposures and estimate each individual’s critical windows and distributed lag effects. To answer these questions, we consider heterogeneous distributed lag effects that differ across a set of modifying covariates specific to each observation. Potential modifiers in our analysis include continuous variables: maternal age and body mass index (BMI); ordinal variables: income classification, highest educational attainment, and smoking (never, former, less than 10 cigarettes/day, at least 10 cigarettes/day); nominal variables: marital status, prenatal care, and race; and binary variables: sex and Hispanic indicators. The distribution of the modifiers are described in Supplementary Materials Section 1.

At each census tract in our study, daily $\text{PM}_{2.5}$ measurements were obtained from EPA community multiscale air quality modeling system (CMAQ) using downscaled data (Berrocal et al., 2010). We then created 37 consecutive weekly average exposures for each pregnancy beginning on the date of conception for the census tract of residence. The weekly average $\text{PM}_{2.5}$ data were log-transformed to reduce skew. The weekly average log-transformed $\text{PM}_{2.5}$ measurements range from 0.68 to 3.53 with mean 1.97 and standard deviation 0.30. Pregnancy average log $\text{PM}_{2.5}$ exposure ranged from 1.34 to 2.33. To account for potential spatial and temporal confounding, we included a fixed intercept for county, year, and month of conception, and controlled for census tract elevation and trimester average temperature. This study was approved by the Institutional Review Board of Colorado State University.

3 Methods

3.1 Heterogeneous DLM Framework

We consider a sample $i = 1, \dots, n$ with continuous outcome y_i , a vector of exposure measurements $\mathbf{x}_i = [x_{i1}, \dots, x_{iT}]'$ taken at equally spaced times $t \in \{1, \dots, T\}$, and a vector

of covariates, \mathbf{z}_i , which includes the model intercept. In this paper, y_i refers to BWGAZ while x_{it} is the $\text{PM}_{2.5}$ exposure measurement for individual i during week t of pregnancy (considering $T = 37$ weeks of gestation). When there is no heterogeneity in the exposure effect across the sample population, the discrete time DLM takes the form

$$y_i = \sum_{t=1}^T x_{it}\theta_t + \mathbf{z}_i'\boldsymbol{\gamma} + \varepsilon_i. \quad (1)$$

Here, θ_t represents the linear effect due to exposure at time t , $\boldsymbol{\gamma}$ is a vector of regression coefficients and ε_i represents independent errors distributed $\mathcal{N}(0, \sigma^2)$.

We consider a DLM where the exposure effects $\theta_1, \dots, \theta_T$ vary across the population. Let the modifiers, \mathbf{m}_i , be a subset of the covariates, \mathbf{z}_i . The heterogeneous DLM is

$$y_i = \sum_{t=1}^T x_{it}\theta_t(\mathbf{m}_i) + \mathbf{z}_i'\boldsymbol{\gamma} + \varepsilon_i \quad (2)$$

where $\theta_t(\mathbf{m}_i)$ is the exposure effect at time t specific to an observation with modifiers \mathbf{m}_i .

Our method for modeling heterogeneity due to a set of modifying covariates uses an ensemble of regression trees combined with functional estimators of the distributed lag effect. We denote a modifier regression tree by \mathcal{M}_a for $a \in \{1, \dots, A\}$ that partitions the population based on a set of modifiers \mathbf{m}_i . Terminal nodes are denoted η_{ab} where $b = 1, \dots, B_a$ distinguishes the subgroups partitioned by tree a . Each terminal node is associated with a T -dimensional vector of parameters $\boldsymbol{\theta}_{ab}$. Considering all trees in the ensemble, the distributed lag function for observation i , $\boldsymbol{\theta}(\mathbf{m}_i) = [\theta_1(\mathbf{m}_i), \dots, \theta_T(\mathbf{m}_i)]'$, is

$$\boldsymbol{\theta}(\mathbf{m}_i) = \sum_{a=1}^A \sum_{b=1}^{B_a} \boldsymbol{\theta}_{ab} \mathbb{I}(\mathbf{m}_i \in \eta_{ab}) \quad (3)$$

where $\boldsymbol{\theta}_{ab} = [\theta_{ab1}, \dots, \theta_{abT}]'$ parameterizes the partial distributed lag function for the subgroup represented by terminal node η_{ab} in tree \mathcal{M}_a and $\mathbb{I}(\cdot)$ is the indicator function.

3.2 Gaussian Process HDLM

We first propose a method for estimating the HDLM using Gaussian processes, which is an established approach for DLMs (e.g. Warren et al. (2012)). Consider a single modifier tree terminal node, η_{ab} , containing a subset of observations. Let the corresponding T -dimensional set of DLM parameters $\boldsymbol{\theta}_{ab}$ follow a Gaussian process with covariance function $\Sigma_\phi(t, t')$ where ϕ are parameters defining the covariance. We consider the exponential covariance, $\Sigma_\phi(t, t') = \exp\{-\phi|t - t'|\}$. An inherent assumption of this approach is that all observations share the same value of ϕ and therefore have the same smoothness over time

in their distributed lag effects. Having a common ϕ for all nodes on a tree is required due to model computation, which requires integration over the distributed lag effects for each subgroup. The equal smoothness assumption may be beneficial if the distributed lag effects for all observations have a similar magnitude and window length. In the case where there is a nonzero exposure effect in only a small proportion of the population, the smoothness of the distributed lag effect imposed by the remaining sample will make this critical window difficult to estimate. This is because estimation of the smoothing parameter will largely reflect the null group and cause oversmoothing of the active group.

We define the Gaussian process prior for the distributed lag effects as

$$\boldsymbol{\theta}_{ab}|\tau_a, \nu, \sigma, \phi \sim \mathcal{GP}[\mathbf{0}, \tau_a^2 \nu^2 \sigma^2 \boldsymbol{\Sigma}(\phi)]. \quad (4)$$

The variance parameters follow a half-Cauchy prior, $\tau_a, \nu \sim \mathcal{C}^+(0, 1)$, to define a local-global horseshoe-like estimator on tree specific effects (Carvalho et al., 2010). This differs from previous BART implementations (Chipman et al., 2010; Starling et al., 2020), which apply a uniform variance across all trees. The horseshoe variance prior will shrink the effects of misspecified trees reducing variance and false window detection. A similar prior specification was shown to improve DLM estimation in the treed DLM method of Mork and Wilson (2021a). We restrict the range of ϕ to $\exp\{-\phi\} \in (0.05, 0.95)$ and assign prior $\phi \sim \text{Gamma}(1/2, 1/2)$, which gives higher probability to smoother distributed lag effects.

3.3 Nested Tree HDLM

Mork and Wilson (2021a) showed that treed DLMs outperform competing spline and Gaussian process-based methods in terms of distributed lag effect estimation and precision of critical window identification. We propose using a treed DLM as a parametric model at each terminal node of the modifier tree. This results in a nested tree structure visualized in Figure 1a. Here, each subgroup of the modifier tree is paired with a unique distributed lag tree structure and corresponding effects.

Before describing the nested tree HDLM we give an overview of the treed DLM. The notation presented here distinguishes the DLM regression tree from the modifier regression tree presented in Section 3.1. Consider binary tree \mathcal{D} , which partitions the exposure time span, T , into C non-overlapping time segments. Internal nodes of \mathcal{D} are assigned binary rules at time points within the period of exposure (e.g. $t < t_1$ and $t \geq t_1$ for $t_1 \in \{2, \dots, T\}$). The terminal nodes of \mathcal{D} , denoted λ_c for $c \in \{1, \dots, C\}$, bin together time points to define a piecewise constant distributed lag effect (see Figure 1a). That is, $\theta_t = \delta_c$ if $t \in \lambda_c$, where δ_c is a distributed lag effect for all exposure observations within the time period of λ_c . The binning of distributed lag effects adds structure to the distributed lag function and stabilizes the model in the presence of autocorrelation in the exposure data.

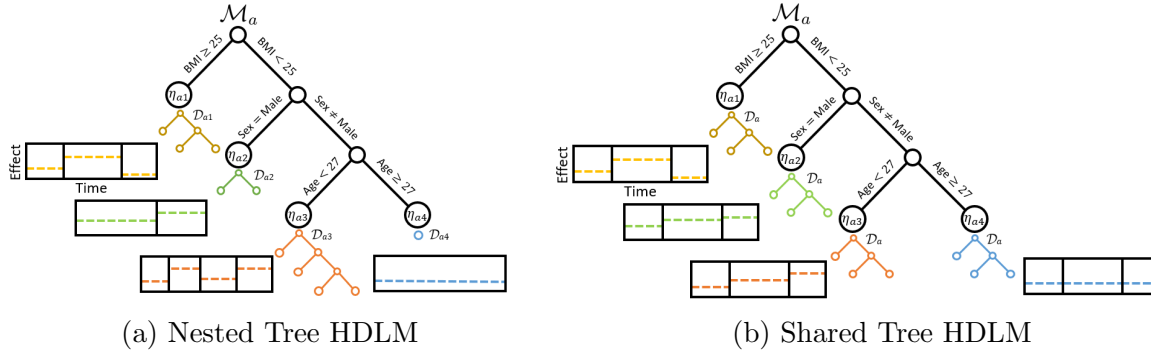


Figure 1: Panel (a) diagrams the nested tree HDLM. Modifier tree \mathcal{M}_a is structured with binary splitting rules on modifiers BMI, sex, and age. Each terminal node η_{ab} has a unique treed DLM structure \mathcal{D}_{ab} with corresponding piecewise effects given by δ_{abc} , shown as dashed lines. Panel (b) diagrams the shared tree HDLM. Here, each terminal node of the modifier tree η_{ab} uses the same treed DLM structure \mathcal{D}_a . The time points where the distributed lag effects change are shared across all trees while the effect magnitude is unique to each subgroup.

In the nested tree DLM, each modifier tree subgroup has a unique treed DLM structure. As a result, there is no sharing of information across terminal nodes concerning the timing of the critical window, the effect size, or the smoothness of the DLM. This creates a highly flexible model that allows structures of the treed DLM to adapt to the subgroup whose exposure-response is being estimated. Keeping the number of treed DLM terminal nodes small introduces constraints in the distributed lag function to account for temporal correlation in the exposure measurements.

To formally define the nested tree DLM in the context of an ensemble of modifier trees, denote \mathcal{D}_{ab} as the treed DLM associated with terminal node η_{ab} in modifier tree \mathcal{M}_a . Treed DLM \mathcal{D}_{ab} contains C_{ab} terminal nodes, denoted λ_{abc} , with corresponding distributed lag effects δ_{abc} , $c = 1, \dots, C_{ab}$. To calculate the HDLM, as in (3), let $\theta_{abt} = \delta_{abc}$ if $\mathbf{m}_i \in \eta_{ab}$ and $t \in \lambda_{abc}$. Then the distributed lag effect for individual i at time t is

$$\theta_t(\mathbf{m}_i) = \sum_{a=1}^A \sum_{b=1}^{B_a} \sum_{c=1}^{C_{ab}} \delta_{abc} \mathbb{I}(\mathbf{m}_i \in \eta_{ab}, t \in \lambda_{abc}). \quad (5)$$

3.4 Shared Tree HDLM

The shared tree HDLM is a simplification of the nested tree HDLM that pairs a single treed DLM with each modifier tree. All subgroups of a modifier tree receive the same treed DLM structure but distributed lag effects with different magnitudes. The shared tree HDLM is visualized in Figure 1b. The modifier tree and treed DLM structures are learned from the data, but a change in the treed DLM structure is applied to all subgroups of a modifier

tree. This assumes that the DLM has the same change points for critical windows. For our data problem involving prenatal development, this could relate to an assumption that developmental stages always occurring during the same weeks, although the magnitude of effects may differ. In contrast, the nested tree HDLM allows for the possibility that the onset and duration of the effects varies for each subgroup.

Notation for the shared tree HDLM is similar to the nested tree HDLM. For each modifier tree \mathcal{M}_a with terminal nodes η_{ab} , we consider a single treed DLM \mathcal{D}_a with terminal nodes λ_{ac} , $c \in \{1, \dots, C_a\}$. The treed DLM \mathcal{D}_a is utilized as the distributed lag function at all terminal nodes η_{ab} of \mathcal{M}_a . The distributed lag effects, δ_{abc} , are specific to each modifier tree terminal node and treed DLM terminal node. As in the nested tree DLM, we calculate the heterogeneous DLM by setting $\theta_{abt} = \delta_{abc}$ if $t \in \lambda_{ac}$.

3.5 Prior Specification

Here we detail the prior specification of nested tree HDLM. The approach for other methods are similar and details are available in Supplementary Materials Section 2. The nested tree HDLM prior consists of five components: modifier tree structure, treed DLM structure, distributed lag effects, fixed effects of covariates, and the error variance. We have several goals in mind when shaping priors. First, as with BART, trees with fewer terminal nodes will help to stabilize the model. This is particularly true for the treed DLM where few terminal nodes provide a necessary constraint on the distributed lag effects. Second, the model should prioritize rules on modifiers that result in different DLM structures or effects to remove modifiers that do not differentiate subgroups. Third, we want to lower false window detection rates by shrinking the effects pertaining to subgroups and treed DLMs that poorly fit the data.

3.5.1 Modifier Tree Priors

The prior on modifier tree structures is defined in two parts: a prior probability that a node will have a split and a prior probability of the binary rule defined at that split. We adopt the BART prior for a node split. That is, for node η with depth d_η (the first node in a tree has depth zero) the probability the node is an internal node equals $p_{\text{split}}(\eta) = \alpha(1 + d_\eta)^{-\beta}$ where $\alpha \in (0, 1)$ and $\beta > 0$. Following Chipman et al. (2010) we set $\alpha = 0.95$ and $\beta = 2$, which encourages smaller trees. Changes to these priors did not improve performance in simulations. Priors on tree splitting rules in the modifier tree follow Linero (2018). Complete details are given in Supplementary Materials Section 2.

3.5.2 Treed DLM Priors

The treed DLM also uses the BART prior for node splits, with $\alpha = 0.95$ and $\beta = 2$. For the splitting rule prior, we assign a uniform prior across all available time points, resulting in $T - 1$ possible splits for a tree with a single node.

The distributed lag effects are assigned the conjugate normal prior,

$$\delta_{abc} | \tau_a, \nu, \sigma \sim \mathcal{N}(0, \tau_a^2 \nu^2 \sigma^2) \quad (6)$$

where $\tau_a, \nu \sim \mathcal{C}^+(0, 1)$ define a horseshoe-like estimator on tree specific effects. We include the error variance σ^2 in this prior, allowing it to be integrated out during tree updates. This prior specification differs from previous BART implementations (Chipman et al., 2010; Starling et al., 2020), which apply a uniform variance prior across all trees. The modifier-tree-specific variance prior improves performance in treed DLM because it shrinks the effects of misspecified trees, which serves to reduce variance and false window detection (Mork and Wilson, 2021a).

3.5.3 Other Priors

To complete a fully Bayesian specification of the nested tree DLM we assign a non-informative prior to the fixed effects, $\gamma \sim \mathcal{MVN}(\mathbf{0}, d\sigma^2 I_p)$, where I_p is a $p \times p$ identity matrix and d is fixed at a large value. Finally, we specify prior $\sigma \sim \mathcal{C}^+(0, 1)$.

3.6 Computation

The nested tree DLM is estimated by sampling from the posterior distribution using MCMC. As in BART, we apply Bayesian backfitting (Hastie and Tibshirani, 2000) to estimate the effects for each modifier tree and apply the independent Metropolis-Hastings (MH) algorithm to update modifier trees and treed DLMs. Our algorithm differs from BART in several ways. First, we control for a set of fixed effects when estimating the heterogeneous DLMs. Second, each terminal node of the modifier tree has a unique treed DLM structure that is learned from the data and must be updated. We briefly outline our algorithm and provide full details in Supplementary Materials Section 3.

To improve estimates of the distributed lag function we integrate the fixed effect parameters, γ , out of the data likelihood. Updates to the modifier tree occur through the four proposal steps described in Chipman et al. (1998): grow, prune, change, and swap. The grow step adds an additional split at a terminal node, and prune removes a split from an internal node connected to two terminal nodes. The change step modifies a binary splitting rule at an internal node. Swap reverses the order of rules in two adjacent internal nodes.

Each terminal node of the modifier tree has a unique treed DLM. In a grow proposal, a terminal node becomes an internal node and the corresponding treed DLM is eliminated and replaced by two new treed DLMs at the new modifier tree terminal nodes. For each new terminal node, a new treed DLM is drawn from the tree prior. Likewise for a prune proposal, an internal node becomes a terminal node. In this case the two existing treed DLMs are discarded and a new treed DLM is drawn from the tree prior. During a change or swap step in the modifier tree the terminal nodes retain the same treed DLM. To account for the potential change in dimensionality during modifier tree updates we integrate over all terminal node effects, δ_{abc} , and model variance, σ^2 . The update can then proceed with a MH step similar to that used in previous BART implementations.

After an update to the modifier tree, we update the treed DLM associated with each subgroup. Updates to treed DLMs use only grow, prune, and change proposals. A swap results in empty treed DLM terminal nodes and is not used. Conditionally conjugate normal priors allow for Gibbs updates of terminal node effects. Following updates to tree structures and terminal node effects, the remaining parameters are updated with standard MCMC procedures.

4 Simulation

We developed three simulation scenarios to evaluate estimation of the heterogeneous distributed lag function and the ability to identify correct modifiers. The first simulation scenario relates to the nested tree HDLM and considered subgroups with three different distributed lag effects: an early window, a late window, and no effect. The second scenario mimics the shared tree HDLM and had two groups: a distributed lag effect that does not change in time but was scaled by a continuous modifier and a group with no effect. Scenario 3 compared the HDLM to traditional DLM methods when there was no effect modification.

In general, we found that the nested and shared tree HDLMs outperform the Gaussian process HDLM in all settings and performed similarly to a standard DLM in scenario 3 with no effect modification. For subgroups with no distributed lag effects, the nested tree HDLM was better than the shared tree HDLM. In a low noise setting we saw a greater distinction between the nested and shared tree approaches, while they were comparable in higher noise scenarios.

Each scenario involved 13 covariates. Two of these covariates were responsible for the DLM heterogeneity in scenarios 1 and 2. All covariates were included as potential modifiers in the HDLMs. Covariates $\mathbf{z}_i = [z_{i1}, \dots, z_{i13}]'$ were independently generated: $z_{i1} \sim \mathcal{N}(0, 1)$, $z_{i2} \sim \text{Bernoulli}(0.5)$, $z_{i3} \sim \text{Uniform}(0, 1)$, $z_{ip} \sim \mathcal{N}(0, 1)$ for $p \in \{4, \dots, 8\}$, $z_{ip} \sim \text{Bernoulli}(0.5)$ for $p \in \{9, \dots, 13\}$. We also include $z_{i0} = 1$ as a model intercept. A

set of 37 consecutive weekly PM_{2.5} exposures, denoted $\mathbf{x}_i = [x_{i1}, \dots, x_{i37}]'$ was drawn for each observation using real exposure measurements from our data analysis.

The simulation generated continuous outcomes under the model

$$y_i = r \cdot \mathbf{x}_i' \boldsymbol{\theta}(\mathbf{m}_i) + \mathbf{z}_i' \boldsymbol{\gamma} + \varepsilon_i \quad (7)$$

where $\boldsymbol{\gamma}$ are parameters drawn from standard normal, and $\boldsymbol{\theta}(\mathbf{m}_i)$ represent the HDLM from each simulation scenario. In the HDLM we let \mathbf{m}_i be all variables in \mathbf{z}_i except for the intercept, although only two modifiers are actually responsible for the effect heterogeneity. Scaling factor r was defined such that $\text{Var}[r \cdot \mathbf{x}_i' \boldsymbol{\theta}(\mathbf{m}_i)] = 1$, and ε_i was drawn independently from $\mathcal{N}(0, \sigma^2)$ under three different noise settings, $\sigma^2 \in \{10, 25, 50\}$. Each simulation scenario and σ^2 combination was run 100 times with $n = 5,000$ observations. An additional 5000 observations were generated as a testing dataset to evaluate out-of-sample model performance but not used for model fitting.

Each simulation replicate was estimated by three methods for HDLM: nested tree HDLM, shared tree HDLM, and Gaussian process HDLM. We also used two methods for a standard DLM: treed DLM and Gaussian process DLM. Simulation scenario 1 was also estimated using the nested tree and Gaussian process HDLM where the modifier tree was fixed to use the true subgroups. All models used 20 modifier trees in the ensemble and were run for 10,000 MCMC iterations thinned to every 5th iteration, following 5,000 burn-in iterations. All simulations can be reproduced with R package `dlmtree`.

4.1 Scenario 1: Early/Late Window

We simulated the heterogeneous distributed lag function with two true modifiers, z_{i1} and z_{i2} ,

$$\theta_t(\mathbf{m}_i) = \begin{cases} \mathbb{I}(t \in [11, 18]) & \text{if } z_{i1} > 0 \text{ and } z_{i2} = 1 \\ \mathbb{I}(t \in [17, 26]) & \text{if } z_{i1} > 0 \text{ and } z_{i2} = 0 \\ 0 & \text{if } z_{i1} \leq 0 \end{cases} \quad (8)$$

The first group ($z_{i1} > 0, z_{i2} = 1$) had a nonzero distributed lag effect during weeks 11 – 18. The second group ($z_{i1} > 0, z_{i2} = 0$) had a nonzero distributed lag effect during weeks 17 – 26, overlapping with the first group by two weeks. The third group ($z_{i1} \leq 0$) had no distributed lag effect.

Pointwise DLM results averaged across simulation replicates are given in Table 1. We separately analyzed subgroups with an effect ($z_{i1} > 0$) from subgroups with no effect ($z_{i1} \leq 0$). We report DLM root mean square error (RMSE) = $\sqrt{\sum_{t=1}^{37} [\theta_t(\mathbf{m}_i) - \hat{\theta}_t(\mathbf{m}_i)]^2 / 37}$ and coverage of the distributed lag effects by 95% pointwise credible intervals, averaged across observations in effect and no effect subgroups. We also calculated the probability

that the model detects a true critical window (true positive, TP) when $\theta_t(\mathbf{m}_i)$ is nonzero as well as the probability a critical window is identified where the true effect is zero (false positive, FP), both using the 95% pointwise credible interval for the distributed lag effects. Finally we report the mean square prediction error (MSPE), $n^{-1} \sum_{i=1}^n (y_i - \hat{y}_i)^2$. We report MSPE as the ratio of MSPE for each model relative to the treed DLM without modification using 5,000 additional out-of-sample observations for each simulation replicate. The MSPE differences are small across all models because the signal of the HDLM is small relative to the fixed effects and residual variance.

Table 1: Simulation results for estimating the DLM in scenario 1 (early/late effect). Results are considered pointwise across the DLM for each individual and broken down for individuals with a zero versus nonzero effect. MSPE is calculated for the response using 5,000 out of sample observations and divided by the MSPE for treed DLM without modification.

Model	Effect ($z_{i1} > 0$)				No Effect ($z_{i1} \leq 0$)			MSPE
	RMSE*	Coverage	TP	FP	RMSE*	Coverage	FP	
$\sigma^2 = 10$								
Nested Tree HDLM	4.36	0.95	0.94	0.02	2.32	1.00	0.00	0.938
Shared Tree HDLM	5.30	0.93	0.94	0.04	2.70	0.99	0.01	0.940
Gaussian Process HDLM	5.63	0.95	0.97	0.02	3.51	0.99	0.01	0.941
Nested Tree: Truth	3.08	0.97	0.98	0.02	1.21	1.00	0.00	0.933
Gaussian Process: Truth	5.24	0.95	1.00	0.03	3.05	1.00	0.00	0.941
Treed DLM	11.26	0.63	0.92	0.20	5.58	0.64	0.36	1.000
Gaussian Process DLM	11.28	0.65	0.84	0.17	5.61	0.69	0.31	0.998
$\sigma^2 = 25$								
Nested Tree HDLM	6.72	0.91	0.88	0.04	2.67	1.00	0.00	0.977
Shared Tree HDLM	7.39	0.90	0.86	0.05	3.18	0.99	0.01	0.978
Gaussian Process HDLM	7.14	0.95	0.90	0.02	3.94	1.00	0.00	0.978
Nested Tree: Truth	5.29	0.96	0.94	0.02	1.96	1.00	0.00	0.974
Gaussian Process: Truth	6.43	0.96	0.97	0.02	3.63	1.00	0.00	0.987
Treed DLM	11.45	0.64	0.84	0.18	5.52	0.68	0.32	1.000
Gaussian Process DLM	11.49	0.70	0.61	0.11	5.55	0.78	0.22	0.999
$\sigma^2 = 50$								
Nested Tree HDLM	9.70	0.80	0.71	0.08	3.37	1.00	0.00	0.993
Shared Tree HDLM	9.86	0.79	0.71	0.09	3.64	0.99	0.01	0.993
Gaussian Process HDLM	9.29	0.90	0.50	0.02	4.30	1.00	0.00	0.992
Nested Tree: Truth	7.26	0.92	0.91	0.04	2.56	1.00	0.00	0.989
Gaussian Process: Truth	7.53	0.96	0.83	0.01	4.04	1.00	0.00	0.990
Treed DLM	11.70	0.66	0.77	0.16	5.39	0.71	0.29	1.000
Gaussian Process DLM	11.73	0.74	0.40	0.06	5.46	0.87	0.13	1.000
RMSE* = RMSE \times 100								

The nested tree HDLM yields distributed lag estimates with smaller RMSE than those from shared tree and Gaussian process HDLMs across all error settings. For critical window identification, the nested tree HDLM yields a similar or higher TP than the other models in all error settings. The FP of the nested tree HDLM ranges from 0.02 in the lowest error setting to 0.08 in the highest error setting; the shared tree HDLM has FP ranging

from 0.04 to 0.09, respectively. The added flexibility of the nested tree HDLM allowed for different change points for critical windows and varying smoothness in the effect and no effect groups, features lacking in the shared tree and Gaussian process HDLMs. Coverage of the distributed lag function was near nominal levels except in the highest error setting, where coverage decreased in all HDLMs. The decreased coverage was only evident in the subgroups with a true exposure effect and is due to two factors: shrinkage of the exposure effect and in some cases combining the two groups with different critical windows into a single group. Coverage in the no effect group was above the nominal level in all settings. The nested tree DLM also had similar or lower MSPE than competing methods.

The treed DLM model with subgroups fixed at the truth outperformed the HDLM models. However, the fixed subgroup Gaussian process approach had higher RMSE and MSPE than the nested tree HDLM in the lowest error scenario. This is first due to the fact that the true distributed lag function is not smooth. Second, the smoothness assumption of the Gaussian process was homogeneous across all subgroups, leading to over-smoothing in the effect subgroups and under-smoothing in the no effect subgroup. These results motivate the use of the treed DLM approaches when considering heterogeneity. The DLM methods with no effect modification were consistently the worst performing models with low coverage of the distributed lag function, higher FP rates, and the highest RMSE and MSPE.

In Supplementary Materials Section 4 we present modifier posterior inclusion probabilities (PIP) for an individual modifier or interactions of modifiers. The PIP for an individual modifier is the probability that the modifier is used in at least one splitting rule across the ensemble of trees. We define a modifier interaction to be when two modifiers are used as consecutive splitting rules in the same tree. The average modifier PIPs will be a function of the number of modifiers and number of trees in the model with larger PIPs for fewer modifier or more trees. Modifiers with a larger PIP relative to other modifiers represent possible modification of the distributed lag effects and critical windows, and give a starting point to comparing the exposure effects for individuals or subgroups.

In scenario 1, the true modifiers (z_1 and z_2) have PIPs that range from 0.97 to 1 in the low and middle noise scenarios and 0.79 to 0.99 in the high noise scenario. The other modifiers have PIPs ranging from 0.59 to 0.63, on average. The modifier that determines the critical window placement, z_2 has slightly lower PIP than the modifier that determines effect versus no effect groups, z_1 . For scenario 1, we found an interaction between modifiers z_1 and z_2 to have PIP of 1 in the low error setting, 0.88 in the middle error setting, and 0.46 in the highest error setting. The average PIP for other modifier interactions was 0.11. We note that a model with more trees or fewer modifiers would likely find higher PIPs for irrelevant modifiers because there are more chances for a splitting rule to use each modifier.

4.2 Scenario 2: Scaled Effect

In scenario 2 we simulated the heterogeneous distributed lag function based on two continuous covariates z_{i1} and z_{i3} ,

$$\theta_t(\mathbf{m}_i) = \begin{cases} z_{i3}\mathbb{I}(t \in [11, 18]) & \text{if } z_{i1} > 0 \\ 0 & \text{if } z_{i1} \leq 0 \end{cases}. \quad (9)$$

The distributed lag function is nonzero during weeks 11 – 18 for the first group ($z_{i1} > 0$) and scaled by the modifier z_{i3} . The second group ($z_{i1} \leq 0$) had no distributed lag effects. Here, we did not compare to a fixed subgroups model because the continuous modification does not allow for true subgroups.

Table 2 summarizes model performance in term of estimation of the distributed lag function and out-of-sample MSPE. The shared tree HDLM yielded lower RMSE on the distributed lag function in low and middle error settings, higher TP rate for identifying windows, and similar MSPE compared to other HDLM approaches. The added flexibility of the nested tree model was not needed, which leads to slightly lower performance of this approach in this scenario. In order for the Gaussian process model to perform better, the smoothness of the DLM would need to vary due to the modifier z_3 , which is not possible in the current method.

Supplementary Materials Section 4 presents PIPs for individual modifiers and modifier interactions. The modifier tree HDLMs correctly distinguish the true modifiers in all error settings with PIPs ranging from 0.87 to 1. The other modifiers have PIPs ranging from 0.55 to 0.63, on average. In the highest error setting the modifier responsible for effect size change, z_3 , has slightly lower PIP (0.88) than the modifier responsible for effect or no effect subgroups, z_1 (1). We found the interaction between modifiers z_1 and z_3 to have PIP of 1 in the low error setting, 0.91 in the middle error setting, and 0.65 in the highest error setting. The average PIP for other modifier interactions was 0.11.

4.3 Scenario 3: No Effect Heterogeneity

In the final simulation scenario we considered a DLM without effect modification. The distributed lag effects were defined $\theta_t(\mathbf{m}_i) = \max[0, (t - s)(s - t + 9)]$, where s is a starting time drawn uniformly from $\{1, \dots, T - 9\}$. That is, the distributed lag function is smooth with a critical window over an 8-week time period. The distributed lag effect is identical for all observations in a given dataset.

Table 3 presents results for estimation of the distributed lag function. The HDLM performs on par with standard DLM methods without heterogeneity. The HDLM methods have higher RMSE than the standard TDLM and similar to the Gaussian process DLM.

Table 2: Simulation results for estimating the DLM in scenario 2 (scaled effect). Results are considered pointwise across the DLM for each individual and broken down for individuals with a zero versus nonzero effect. MSPE is calculated for the response using 5,000 out of sample observations.

Model	Effect ($z_{i1} > 0$)				No Effect ($z_{i1} \leq 0$)			MSPE
	RMSE*	Coverage	TP	FP	RMSE*	Coverage	FP	
$\sigma^2 = 10$								
Nested Tree HDLM	5.05	0.92	0.77	0.01	2.30	0.99	0.01	0.920
Shared Tree HDLM	4.60	0.93	0.86	0.01	2.37	0.99	0.01	0.919
Gaussian Process HDLM	6.23	0.94	0.69	0.02	3.58	1.00	0.00	0.923
Treed DLM	10.37	0.81	0.97	0.01	6.04	0.78	0.22	1.000
Gaussian Process DLM	10.71	0.82	0.99	0.02	5.94	0.77	0.23	1.000
$\sigma^2 = 25$								
Nested Tree HDLM	6.62	0.92	0.66	0.01	2.59	1.00	0.00	0.969
Shared Tree HDLM	6.53	0.93	0.76	0.01	2.85	0.99	0.01	0.969
Gaussian Process HDLM	7.53	0.94	0.63	0.01	3.98	1.00	0.00	0.971
Treed DLM	10.92	0.82	0.92	0.02	5.72	0.78	0.22	1.000
Gaussian Process DLM	11.12	0.84	0.86	0.01	5.71	0.80	0.20	1.000
$\sigma^2 = 50$								
Nested Tree HDLM	8.48	0.91	0.62	0.01	3.10	1.00	0.00	0.986
Shared Tree HDLM	8.59	0.91	0.64	0.02	3.42	0.99	0.01	0.987
Gaussian Process HDLM	9.02	0.93	0.53	0.00	4.26	1.00	0.00	0.988
Treed DLM	11.54	0.81	0.86	0.03	5.30	0.79	0.21	1.000
Gaussian Process DLM	11.54	0.85	0.58	0.01	5.44	0.87	0.13	1.000
RMSE* = RMSE \times 100								

Coverage of the true distributed lag effects by 95% pointwise credible intervals meet the nominal level. The TP rates from the HDLM methods are slightly below those from the DLM methods without effect heterogeneity while the FP rate is near zero for all methods. The tree-based HDLMs outperformed the Gaussian process DLM in the higher noise setting; these results encourage the use of tree-based approaches for estimating a DLM or HDLM in general. In terms of modifier selection, the average PIP of any given modifier ranges from 0.63 to 0.69. This is similar to the non-active modifiers in simulation scenarios 1 and 2. Full details of modifier inclusion are given in Supplementary Materials Section 4.

5 Data Analysis

We applied the nested tree, shared tree, and Gaussian process HDLMs to estimate the relationship between BWGAZ and a mother’s exposure to PM_{2.5} during the first 37 weeks of pregnancy. We allowed for effect heterogeneity due to ten modifiers and controlled for all demographic, spatial, and temporal covariates described in Section 2. The covariates and modifiers are outlined in Table 4. We did not include a fixed effect for fetal sex as the outcome, BWGAZ, was already adjusted for this factor. Each model ran for 15,000

Table 3: Simulation results for estimating the DLM in scenario 3 (no effect heterogeneity). Results are considered pointwise across the DLM for each individual. MSPE is calculated for the response using 5,000 out of sample observations and divided by the MSPE for TDLM without modification.

Model	RMSE $\times 100$	Coverage	TP	FP	MSPE
$\sigma^2 = 10$					
Nested Tree HDLM	2.90	0.93	0.83	0.00	1.001
Shared Tree HDLM	2.83	0.94	0.83	0.00	1.001
Gaussian Process HDLM	2.86	1.00	0.94	0.00	1.001
Treed DLM	2.37	0.97	0.89	0.01	1.000
Gaussian Process DLM	2.81	0.99	0.96	0.01	1.007
$\sigma^2 = 25$					
Nested Tree HDLM	3.42	0.97	0.76	0.00	1.001
Shared Tree HDLM	3.35	0.97	0.76	0.00	1.001
Gaussian Process HDLM	3.84	1.00	0.76	0.00	1.001
Treed DLM	3.01	0.98	0.82	0.01	1.000
Gaussian Process DLM	3.64	0.99	0.89	0.01	1.003
$\sigma^2 = 50$					
Nested Tree HDLM	4.31	0.98	0.65	0.00	1.001
Shared Tree HDLM	4.21	0.98	0.67	0.00	1.001
Gaussian Process HDLM	4.73	1.00	0.54	0.00	1.001
Treed DLM	3.76	0.97	0.79	0.01	1.000
Gaussian Process DLM	4.41	0.99	0.80	0.01	1.001

iterations after 5,000 burn-in and was thinned to every 5th iteration. Following a 10-fold cross-validation, the shared tree HDLM had slightly lower MSPE. Because the results from the nested tree HDLM were similar, we defaulted to the shared tree HDLM for the data analysis presented in the main text because it is a simpler model. The Gaussian process HDLM had higher MSPE and higher uncertainty in the DLM estimates. Results of our cross-validation and results from the nested tree and Gaussian process HDLMs are provided in Supplementary Materials Section 5. For comparison, we also modeled the exposure-time-response using a treed DLM without effect modification.

5.1 DLM without effect modification

Figure 2 shows the estimated exposure effect using a treed DLM with no effect modification. We found that increased PM_{2.5} exposure was associated with decreased BWGAZ during each week of gestation. The DLM identifies critical windows during weeks 5-6 and 31-34. The cumulative effect of an inter-quartile range (IQR) increase in PM_{2.5} at every week of pregnancy corresponds to a decrease in BWGAZ of -0.026 (95% CI: $-0.044, -0.006$). In a more interpretable context, an increase from 5.9 to 8.5 $\mu\text{g}/\text{m}^3$ PM_{2.5} (the 25th and 75th weekly exposure percentiles) relates to an approximate decrease in birth weight of 11.3g; this is approximate because BWGAZ adjusts for sex and gestational age.

Table 4: Covariates included as fixed effects or modifiers (indicated by checks) of the HDLM. For covariates included as modifiers we report the posterior inclusion probability (PIP), which is defined as the probability the modifier is used in at least one splitting rule in the ensemble.

Covariate	Type	Mean (IQR)	Categories	Fixed effect	Modifier	PIP
Age at conception	Continuous	28.7 (24 – 33)		✓	✓	0.93
Height	Continuous	64.4 (62 – 66)		✓		—
Prior weight	Continuous	151.3 (126 – 169)		✓		—
Body mass index	Continuous	25.7 (21.6 – 28.4)		✓	✓	0.95
Avg. temp/trimester	Continuous	51.6 (38.2 – 65.1)		✓		—
Income range	Ordinal		6	✓	✓	0.74
Highest education	Ordinal		5	✓	✓	0.90
Smoking habits	Ordinal		4	✓	✓	0.78
Marital status	Categorical		6	✓	✓	0.50
Prenatal care	Categorical		3	✓	✓	0.48
Race	Categorical		4	✓	✓	0.61
County of residence	Categorical		12	✓		—
Month of conception	Categorical		12	✓		—
Year of conception	Categorical		9	✓		—
Hispanic	Binary		2	✓	✓	0.95
Sex of child	Binary		2		✓	0.64

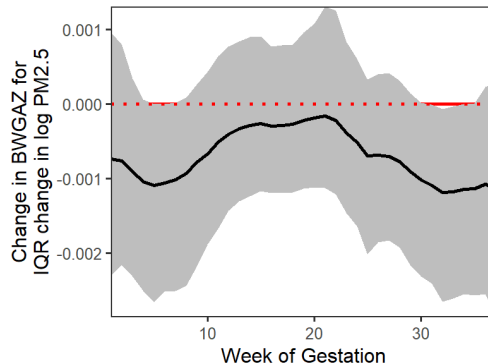


Figure 2: Estimated distributed lag effects due to an IQR increase in $PM_{2.5}$ using the treed DLM with no effect modification. The solid line indicates the posterior mean while the gray area represents a 95% credible interval. Weeks where the credible interval does not contain zero represent critical windows.

5.2 Modifier selection to determine susceptible populations

The modifier PIPs from the shared tree HDLM are presented in Table 4. The modifiers with the highest PIP include maternal BMI (0.95), Hispanic (0.95), age (0.93) and education (0.90). The next highest PIP modifiers were smoking (0.78) and income (0.74). Considering empirical evidence from our simulation scenarios, with a similar number of modifiers and trees, PIPs below 0.7 do not provide significant evidence of effect modification. For continuous modifiers, Figure 3a describes the density of splitting values for age and BMI, with modes at 27 and 22.8, respectively.

Figure 3b illustrates the PIP of interactions between modifiers. In simulation, the

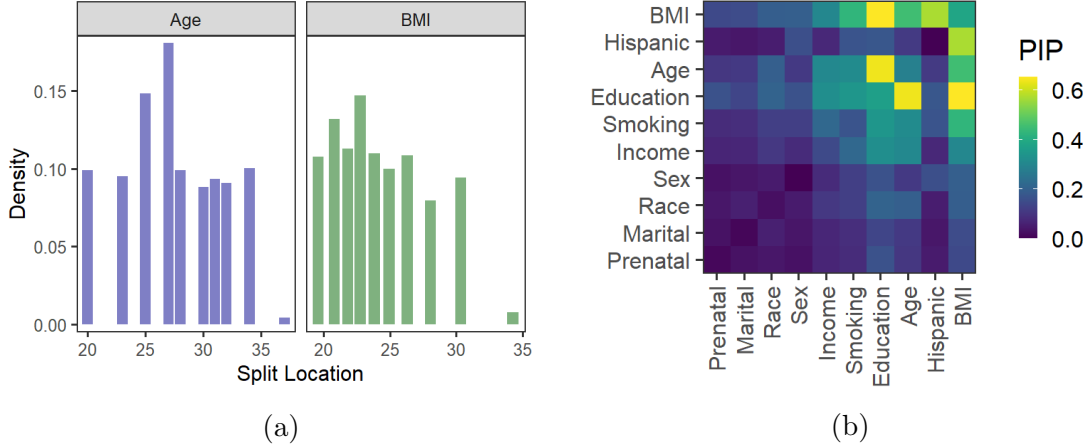


Figure 3: Panel (a) shows the density of splitting locations for two continuous modifiers: maternal age and BMI. Panel (b) shows posterior inclusion probability (PIP) of modifier interactions.

average PIP for non-active modifier interactions was 0.11. We found the highest interaction PIPs to be education–BMI (0.65), education–age (0.64), and BMI–Hispanic (0.57).

When we consider effect modification, we can interpret the effect heterogeneity as an interaction between the modifiers and the exposure effect. For instance, a subgroup that is the result of a rule on a single modifier (59% of tree-specified subgroups) is a two-way interaction between that modifier and $\text{PM}_{2.5}$. The distributed lag effects for a subgroup that is the result of rules on two modifiers (33% of tree-specified subgroups) is a three-way interaction between the two modifiers as well as exposure to $\text{PM}_{2.5}$. While the ensemble of trees should be able to incorporate interactions via the additive nature of multiple trees, some complex interactions, such as the effect/no effect partition in our simulations, may only be captured with a single tree that splits on multiple modifiers.

The modifier PIPs provide a starting point to explore potential susceptible populations, which are characterized by their differential effects to exposure. In this analysis, we focus on four modifiers: maternal BMI, Hispanic, age, and education, along with interactions between these modifiers. To simplify visualization of the results, we divided continuous modifiers, BMI and age, at the splitting value modes. We present subgroup specific average effects along with personalized distributed lag effect estimates for a sample of individuals in each subgroup to give a sense of the remaining within-group heterogeneity.

5.3 Subgroup-specific distributed lag effects

Figures 4a and 5a compare subgroup-specific DLM estimates across pairs of modifiers using the posterior analysis technique described in Supplementary Materials Section 3.5. These subgroups are based on some of the largest modifier PIPs. Other two-way combinations

showed little or no evidence of different subgroup distributed lag effects. More complex multi-way interactions are presented in Supplemental Material Section 5. A consistent theme across subgroup analyses is a differential effect for Hispanic and non-Hispanic subgroups. We see a consistent negative exposure effect at all time points for the non-Hispanic groups and an early and late critical window that is present in many non-Hispanic subgroups. For Hispanic subgroups the exposure effect hovers around zero, which is generally consistent with no exposure effect.

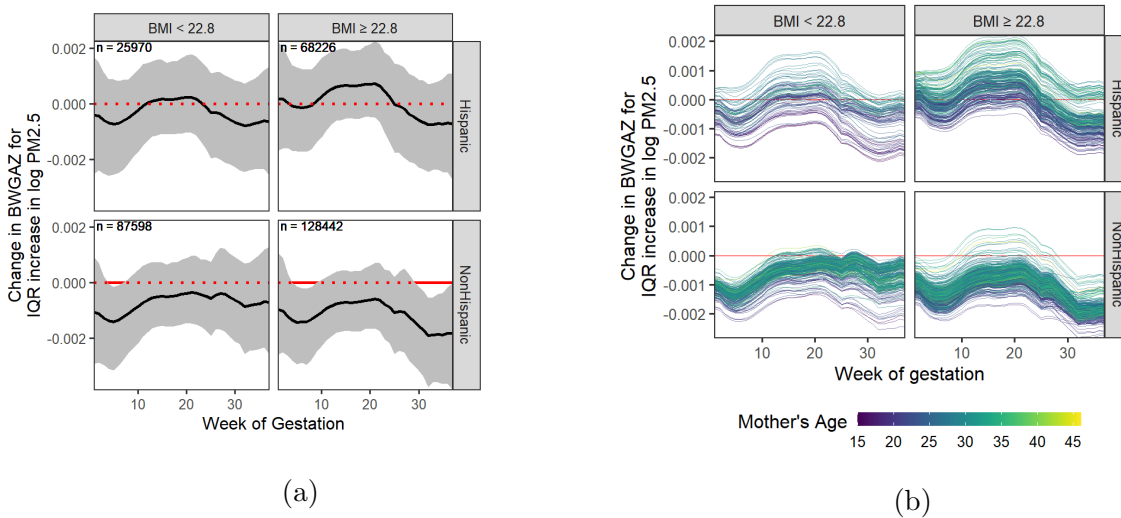
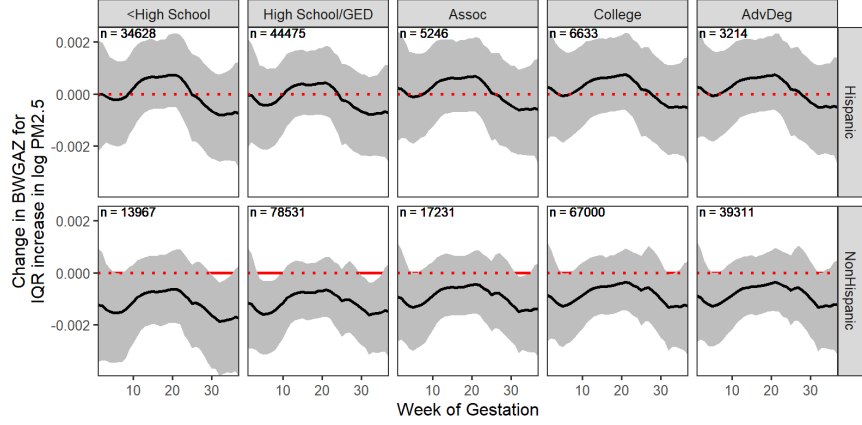


Figure 4: Panel (a) shows subgroup-specific DLM estimates with 95% credible intervals. Panel (b) shows DLM estimates for 1,000 individuals from our data analysis. Both panels are grouped by Hispanic designation (rows) and BMI above/below 22.8 (columns). Panel (b) DLMs are colored according to a Mother's age at conception with lighter color representing older individuals.

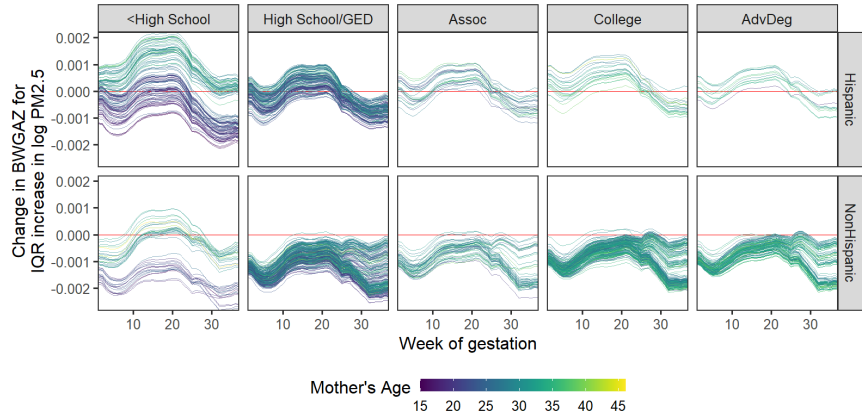
Figure 4a offers evidence of early-gestation susceptibility among all non-Hispanics. For non-Hispanics with BMI above 22.8, we detect a second critical window later in gestation during which increased $PM_{2.5}$ exposure is associated with lower birth weight. We also find differences in critical windows among non-Hispanics based on their level of education, seen in Figure 5a. Non-Hispanics with less than a college education show a late-gestation critical window. Having at most a high school education suggests the presence of an early-gestation critical window for non-Hispanics. For Hispanics, there is no evidence of an association at any level of education.

5.4 Personalized distributed lag effect estimates

The subgroup analysis in Section 5.3 highlights broad trends across modifiers and identifies several susceptible subgroups: non-Hispanic, BMI above 22.8, and less than college



(a)



(b)

Figure 5: Panel (a) shows subgroup-specific DLM estimates with 95% credible intervals, divided by Hispanic and education modifiers. Panel (b) shows DLM estimates for 1,000 individuals from our data analysis divided by Hispanic and education modifiers and colored by age, with lighter color representing older women.

education. However, so far we have considered only two variables at a time. In reality, the individuals in these subgroups vary across the entire observed range of the other modifiers considered in this analysis. In this section, we explore remaining variability in the distributed lag effects among individuals within these subgroups.

Figures 4b and 5b show the estimated DLMs for 1,000 individuals randomly selected from our data set. Estimates for these individuals have been grouped according to the subgroup analysis in Section 5.3 and colored to highlight differences in the distributed lag effects according to a third modifier. This third modifier was selected based on noticeable variation in distributed lag effects among individuals; however, other modifiers are also responsible for these differences.

Figure 4b colors the average distributed lag effects based on the age of the individual

with darker color representing younger mothers. We see a trend towards younger individuals having a larger negative effect. This difference by age is more noticeable for Hispanics with younger individuals showing a more consistently negative effect. Figure 5b visualizes differences by education and Hispanic designation with color again representing continuous modification by maternal age. The distributed lag effects show pronounced differences between younger and older individuals with less than a high school degree. Compared to their older counterparts, young Hispanic and non-Hispanic women with less than a high school education have consistently larger negative effects. Younger women with less education appear to be a highly susceptible group to $PM_{2.5}$ exposure.

5.5 Cumulative effect estimates and four-way interactions

We next explored the differences in total exposure susceptibility across three modifiers simultaneously: maternal BMI, age, and Hispanic designation. We randomly selected 5,000 individuals from our data set and calculated the cumulative effect, or the sum of week-specific effects associated with an IQR increase in $PM_{2.5}$ exposure throughout pregnancy. The estimated cumulative effect was averaged across bins of the continuous modifiers, BMI and age. Results are visualized in Figure 6. For non-Hispanic individuals, higher BMI and lower age correspond to the larger negative effects. Individuals who are older and have lower BMI had the smallest cumulative effect of $PM_{2.5}$. Consistently across the non-Hispanic subgroup, increased exposure was related to lower BWGAZ. For Hispanic individuals, the cumulative effect of exposure was centered around zero. We see evidence of a larger negative effect of exposure for younger Hispanic women; however this effect is less than the cumulative effect for non-Hispanics of the same age and BMI. There is little evidence of modification by BMI for Hispanics.

The cumulative effect of $PM_{2.5}$ exposure on BWGAZ for non-Hispanic individuals in this sample ranged from -0.079 to 0.007 , while for Hispanic individuals the cumulative effect ranged from -0.052 to 0.051 . In the context of birth weight, the cumulative effect of an IQR increase in $PM_{2.5}$ exposure ranges from $-34.3g$ to $3.2g$ for non-Hispanic individuals in the sample and from $-22.8g$ to $22.1g$ for Hispanic individuals. These ranges are approximate because BWGAZ is adjusted for sex and gestational age.

5.6 Model utility

In contrast to the population average effect described in Section 5.1, the HDLM analysis finds evidence of heterogeneity across the population. In particular, we identified several subgroups with increased susceptibility to $PM_{2.5}$ exposure. These susceptible subgroups include non-Hispanic mothers who are younger or have higher BMI as well as non-Hispanic

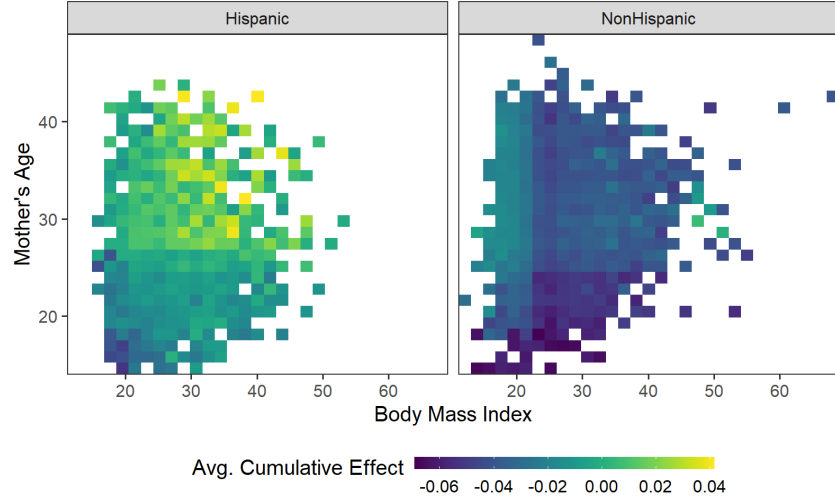


Figure 6: Heat map of average cumulative exposure effect for 5,000 individuals from data analysis. Each colored block is the average cumulative effect for individuals with a particular body mass index (x-axis), age (y-axis) and Hispanic designation (panels). Darker color indicates a larger negative effect on BWGAZ associated with an IQR increase in $PM_{2.5}$ exposure throughout pregnancy.

mothers with lower educational attainment. Using HDLM, we isolated critical windows for these subgroups finding early- and late-gestation to be time periods of higher susceptibility. A personalized analysis found additional variability within the subgroups due to the remaining modifiers. Critical windows for some individuals were much wider than suggested by the population average effect, and for other individuals there was little evidence of any exposure effects. The cumulative effect estimates showed a wide range of variability in the total change in birth weight due to increased $PM_{2.5}$ exposure. Compared to the population average, some individuals showed a 3 times larger decrease in birth weight due to an IQR increase in $PM_{2.5}$ exposure across pregnancy. For susceptible individuals or populations, the HDLM gives the ability to create targeted interventions for precision environmental health. Personalized understanding of exposure effects on health also gives rise to streamlined scientific understanding of biological mechanisms due to exposure.

6 Discussion

We proposed a framework for estimating effect heterogeneity in a distributed lag function due to a possibly high dimensional set of individual modifiers. HDLM can estimate personalized critical windows and effect sizes as well as perform modifier variable selection. In addition, we extend the BART framework by allowing for modification in a multivariate predictor and define the nested tree model composed of one regression tree for modification

and a second regression tree unique to a subgroup for estimating the distributed lag effects.

The nested tree and shared tree HDLMs outperform the Gaussian process HDLM in a simulation study. When effect heterogeneity exists, all HDLM methods outperform methods that assume homogeneity in the distributed lag effects, especially in subgroups with no effect. The difference between standard DLM and HDLM highlights the bias incurred in estimating the distributed lag function both for individuals with and without exposure effects. We also show that our methods consistently estimate high PIPs for modifiers responsible for changes in the distributed lag effects relative to the other potential modifiers. This differentiation in PIPs provides a pathway for selecting modifiers to explore when applying this method. Additional testing of our model suggested modifier selection is insensitive to misspecification of the fixed effects.

We applied the shared tree HDLM to estimate personalized distributed lag effects due to PM_{2.5} exposure in a Colorado, USA birth cohort. This analysis considered ten modifiers of different data types. The model identified four potential modifiers and posterior analysis showed variations in the distributed lag effects for different levels of these modifiers. In particular, we note changes in a late-term critical window due to BMI, overall changes in magnitude due to Hispanic designation, and larger negative effects for young individuals with less than a high school education. We also explored strategies to summarize subgroup-specific distributed lag effects to compare broad differences across the population.

Our proposed methods for estimating an HDLM provide new approaches to exploring individual differences in an exposure-time-response. These tools can lead to personalized environmental health decision making and pinpoint at-risk individuals for intervention. Furthermore, personalized exposure-response functions provide stakeholders with detailed information regarding the burden of air pollution on health.

SUPPLEMENTARY MATERIAL

Supplement: Technical derivations, additional simulation and data analysis results. (PDF)

R-package dlmtree: Code to replicate the simulations available at bit.ly/dlmtree.

References

- Bell, M. L., Ebisu, K., and Belanger, K. (2007). Ambient Air Pollution and Low Birth Weight in Connecticut and Massachusetts. *Children's Health*, 115(7):1118–1124.
- Berrocal, V. J., Gelfand, A. E., and Holland, D. M. (2010). A spatio-temporal downscaler for output from numerical models. *Journal of Agricultural, Biological, and Environmental Statistics*, 15(2):176–197.

- Bose, S., Chiu, Y. H. M., Hsu, H. H. L., Di, Q., Rosa, M. J., Lee, A., Kloog, I., Wilson, A., Schwartz, J., Wright, R. O., Cohen, S., Coull, B. A., and Wright, R. J. (2017). Prenatal nitrate exposure and childhood asthma. Influence of maternal prenatal stress and fetal sex. *American Journal of Respiratory and Critical Care Medicine*, 196(11):1396–1403.
- Carvalho, C. M., Polson, N. G., and Scott, J. G. (2010). The horseshoe estimator for sparse signals. *Biometrika*, 97(2):465–480.
- Chipman, H. A., George, E. I., and McCulloch, R. E. (1998). Bayesian CART model search. *Journal of the American Statistical Association*, 93(443):935–948.
- Chipman, H. A., George, E. I., and McCulloch, R. E. (2002). Bayesian treed models. *Machine Learning*, 48(1-3):299–320.
- Chipman, H. A., George, E. I., and McCulloch, R. E. (2010). BART: Bayesian additive regression trees. *Annals of Applied Statistics*, 4(1):266–298.
- Chiu, Y.-H. M., Hsu, H.-H. L., Coull, B. A., Bellinger, D. C., Kloog, I., Schwartz, J., Wright, R. O., Wright, R. J., Kravis, M., Hospital, C., and Author, E. I. (2016). Prenatal Particulate Air Pollution and Neurodevelopment in Urban Children: Examining Sensitive Windows and Sex-specific Associations HHS Public Access Author manuscript. *Environ Int*, 87:56–65.
- Deshpande, S. K., Bai, R., Balocchi, C., and Starling, J. E. (2020). VCBART: Bayesian trees for varying coefficients. *arXiv preprint arXiv:2003.06416*, pages 1–44.
- Fenton, T. R. and Kim, J. H. (2013). A systematic review and meta-analysis to revise the Fenton growth chart for preterm infants. *BMC Pediatrics*, 13(1).
- Gasparrini, A., Armstrong, B., and Kenward, M. G. (2010). Distributed lag non-linear models. *Statistics in Medicine*, 29(21):2224–2234.
- Hastie, T. and Tibshirani, R. (2000). Bayesian Backfitting. *Statistical Science*, 15(3):196–223.
- Krimsky, S. (2017). The unsteady state and inertia of chemical regulation under the US Toxic Substances Control Act. *PLoS Biology*, 15(12):1–10.
- Lee, A., Hsu, H.-H. L., Chiu, Y.-H. M., Bose, S., Rosa, M. J., Kloog, I., Wilson, A., Schwartz, J., Cohen, S., Coull, B. A., Wright, R. O., and Wright, R. J. (2017). Prenatal fine particulate exposure and early childhood asthma: Effect of maternal stress and fetal sex. *Journal of Allergy and Clinical Immunology*, 141(5):1880–1886.

- Linero, A. R. (2018). Bayesian Regression Trees for High-Dimensional Prediction and Variable Selection. *Journal of the American Statistical Association*, 113(522):626–636.
- Mork, D. and Wilson, A. (2021a). Estimating Perinatal Critical Windows to Environmental Mixtures via Structured Bayesian Regression Tree Pairs. *arXiv preprint arXiv:2102.09071*, pages 1–27.
- Mork, D. and Wilson, A. (2021b). Treed distributed lag non-linear models. *Biostatistics*, *in press*.
- Odden, M. C., Rawlings, A. M., Khodadadi, A., Fern, X., Shlipak, M. G., Bibbins-Domingo, K., Covinsky, K., Kanaya, A. M., Lee, A., Haan, M. N., Newman, A. B., Psaty, B. M., and Peralta, C. A. (2020). Heterogeneous Exposure Associations in Observational Cohort Studies: The Example of Blood Pressure in Older Adults. *American Journal of Epidemiology*, 189(1):55–67.
- Šrám, R. J., Binková, B., Dejmek, J., and Bobak, M. (2005). Ambient air pollution and pregnancy outcomes: A review of the literature. *Environmental Health Perspectives*, 113(4):375–382.
- Starling, J. E., Murray, J. S., Carvalho, C. M., Bukowski, R. K., and Scott, J. G. (2020). Bart with targeted smoothing: An analysis of patient-specific stillbirth risk. *Annals of Applied Statistics*, 14(1):28–50.
- Stieb, D. M., Chen, L., Eshoul, M., and Judek, S. (2012). Ambient air pollution, birth weight and preterm birth: A systematic review and meta-analysis. *Environmental Research*, 117:100–111.
- Warren, J., Fuentes, M., Herring, A., and Langlois, P. (2012). Spatial-Temporal Modeling of the Association between Air Pollution Exposure and Preterm Birth: Identifying Critical Windows of Exposure. *Biometrics*, 68(4):1157–1167.
- Warren, J. L., Luben, T. J., and Chang, H. H. (2020). A spatially varying distributed lag model with application to an air pollution and term low birth weight study. *Journal of the Royal Statistical Society Series C*, 69(3):681–696.
- Wilson, A., Chiu, Y.-H. M., Hsu, H.-H. L., Wright, R. O., Wright, R. J., and Coull, B. A. (2017). Bayesian distributed lag interaction models to identify perinatal windows of vulnerability in children’s health. *Biostatistics*, 18(3):537–552.
- Wright, R. O. (2017). Environment, susceptibility windows, development, and child health.

Zanobetti, A., Wand, M. P., Schwartz, J., and Ryan, L. M. (2000). Generalized additive distributed lag models: quantifying mortality displacement. *Biostatistics*, 1(3):279–292.